Evidence for a significant urbanization effect on climate in China

Liming Zhou*†, Robert E. Dickinson*, Yuhong Tian*, Jingyun Fang‡, Qingxiang Li§, Robert K. Kaufmann¶, Compton J. Tucker‖, and Ranga B. Myneni¶

*School of Earth and Atmospheric Sciences, Georgia Institute of Technology, Atlanta, GA 30332; ‡Department of Urban and Environmental Sciences, and Key Laboratory for Earth Surface Processes of the Ministry of Education, Peking University, Beijing 100871, People's Republic of China; §National Meteorological Center, China Meteorological Administration, Beijing 100081, People's Republic of China; ¶Department of Geography, Boston University, 675 Commonwealth Avenue, Boston, MA 02215; and ‖Biospheric Sciences Branch, Code 923, National Aeronautics and Space Administration/Goddard Space Flight Center, Greenbelt, MD 20771

Edited by James E. Hansen, Goddard Institute for Space Studies, New York, NY, and approved April 28, 2004 (received for review January 15, 2004)

China has experienced rapid urbanization and dramatic economic growth since its reform process started in late 1978. In this article, we present evidence for a significant urbanization effect on climate based on analysis of impacts of land-use changes on surface temperature in southeast China, where rapid urbanization has occurred. Our estimated warming of mean surface temperature of 0.05°C per decade attributable to urbanization is much larger than previous estimates for other periods and locations. The spatial pattern and magnitude of our estimate are consistent with those of urbanization characterized by changes in the percentage of urban population and in satellite-measured greenness.

Land-use changes from urbanization, creating an urban heat island (UHI), have been suspected as partially being responsible for the observed warming over land during the last few decades because of (*i*) the observed decrease in the diurnal temperature range (DTR) resulting from a larger increase or a smaller decrease in minimum temperature relative to maximum temperature and (*ii*) a lower rate of warming observed over the past 20 years in the lower troposphere compared with the surface (1). The area-weighted average warming effect of UHI over land during the 20th century has been estimated to be <0.06°C per century (1–4) globally and approximately 0.06~0.15°C per century (5, 6) in the U.S. based on differences in temperature trends between rural and urban stations. A much larger estimate of 0.27°C per century in the U.S. has been reported recently (7) by comparing trends in observed and reanalysis surface temperatures over the period from 1950 to 1999.

China has experienced rapid urbanization and dramatic economic growth since its reform process started in late 1978. From 1978 to 2000, China's gross domestic product grew at an average annual rate of 9.5%, compared with 2.5% for developed countries and 5% for developing countries; the number of small towns soared from 2,176 to 20,312, nearly double that of the world average during this period; the number of cities increased from 190 to 663; and the proportion of urban population rose from 18% to 39% (see the *Peopledaily* article at http://english.peopledaily.com.cn/200111/27/eng20011127_85410.shtml and the State Family Planning Commission of China web site at www.sfpc.gov.cn/EN/enews20030320-1.htm). In this article, we present evidence for a significant urbanization effect on climate based on analysis of impacts of land-use changes on surface temperature in southeast China, where most of China's urbanization has occurred.

Data and Methods

The UHI effect has been estimated by comparing observed temperatures in urban stations with those in their surrounding rural stations, but such results largely depend on how rural versus urban stations are classified and whether the data are homogeneous (7–9). Population data often are used to identify a station as urban and rural, but such information generally is out-of-date, and thus satellite measurements of night lights have been substituted recently (8, 9). *In situ* observations suffer from inhomogeneities caused by "nonclimatic" factors such as changes in observation time, instrumentation, location (altitude and latitude), and nonstandard siting (referred to as nonclimatic effects hereafter) (9). These factors could introduce artifacts in long-term observations and rural–urban differences and thus may bias the estimate of UHI. For example, Peterson (9) found no significant impact of UHI in the U.S. after the observed temperature time series were adjusted for such inhomogeneities. The lack of an UHI effect may be caused by micro- and local-scale impacts overwhelming the mesoscale UHI. Industrial sections of towns may well be significantly warmer than rural sites are, but urban meteorological observations are more likely to be made within cool "park islands" than in industrial regions (9). Evidently, the UHI is more complex than usually considered.

Using rural–urban temperature differences to estimate the impacts of urbanization on climate in China may be inappropriate for several reasons. First, most Chinese stations are located in or near cities, with only a few in mountainous or remote regions or on small islands. Although China is comparable in size to the U.S., it has considerably fewer meteorological stations, and each city generally has only one station. For example, each of China's two biggest cities, Beijing and Shanghai, has only one station available in the Chinese network. It is impossible to find a corresponding rural station for most of the urban ones, especially in eastern and southern China. Consequently, if using the rural–urban difference to estimate the UHI, one possibly is comparing temperature between two different urban stations at regional scales or between two different regions at large scales. Furthermore, adjusting spatial and temporal homogeneities for *in situ* observations in China inadvertently may sacrifice the UHI effect because the adjustments often are performed by comparing a target station with its neighbors that generally also are urban stations and are relatively far away. Second, China's rapid urbanization in the past two decades could transfer a station from rural into urban in a very short period. The continuous expansion in urban population and area makes the classification of urban versus rural stations dynamic. Third, Chinese cities have a much higher density of population and urban buildings than do cities in most developed countries. Cities in the U.S. extend many kilometers to suburban areas where people reside and that can have as much vegetation as rural

This paper was submitted directly (Track II) to the PNAS office.

Abbreviations: UHI, urban heat island; DTR, diurnal temperature range; R-1, National Centers for Environmental Prediction/National Center for Atmospheric Research (NCEP/NCAR) Reanalysis; R-2, National Centers for Environmental Prediction/Department of Energy (NCEP/DOE) Atmospheric Model Intercomparison Project (AMIP)-II Reanalysis; NDVI, normalized difference vegetation index.

†To whom correspondence should be addressed at: School of Earth and Atmospheric Sciences, 311 Ferst Drive, Georgia Institute of Technology, Atlanta, GA 30332. E-mail: lmzhou@eas.gatech.edu.

www.pnas.org/cgi/doi/10.1073/pnas.0400357101

areas, whereas Chinese cities have a significantly higher density of population, residential buildings, shopping malls, schools, roads, etc., and much less vegetation than their neighboring rural areas because people live within cities. These unique characteristics could make the UHI effect more pronounced in China than in other countries like the U.S. The first two sections of *Supporting Text*, which is published as supporting information on the PNAS web site, provide the details.

Kalnay and Cai (7) recently introduced a method to estimate the impact of urbanization and other land-use changes on climate by comparing trends in surface temperature recorded by 1,982 meteorological stations with those in the National Centers for Environmental Prediction/National Center for Atmospheric Research (NCEP/NCAR) Reanalysis (R-1) (10). The reanalysis uses the most extensive observations available from a variety of sources including ship, rawinsonde, pibal, aircraft, and satellite, etc., to assimilate these data, with an assimilation system kept unchanged, and has been widely used (10). The R-1 data are influenced strongly by atmospheric vertical soundings of wind and temperature, and surface temperatures are estimated from the atmospheric values (surface observations of temperature, moisture, and wind over land are not used) and thus are not sensitive to changes in land surface (7, 10). Therefore, the differences in surface temperature trends between the observed and R-1 data are postulated to represent the impacts of urbanization and other land-use changes on climate (7).

This method assumes that the quality of R-1 surface air temperatures is satisfactory. One known deficiency with R-1 data is its poor performance in the description of cloudiness and surface moisture, which could bias the computation of the surface energy budget and therefore surface air temperature (11, 12). Increased cloud cover is linked with the worldwide decline in DTR, and increased soil moisture could reduce DTR through enhanced evapotranspiration (11–13). Consequently, differences in clouds and soil moisture between observed and R-1 data could contaminate the UHI estimate. The second deficiency with R-1 data is its poor performance over mountainous regions (7). The model of R-1 has a spatial resolution of 2.5° and thus uses a land surface boundary that is smoother than reality. This smoothing could introduce large biases in the model's altitude or land surface properties relative to the actual meteorological stations and thus in the R-1 temperatures over mountainous areas with varied topography. Trenberth (12) argues that the R-1 does not include effects of changing atmospheric composition such as greenhouse gases and aerosols on radiative forcing. However, the R-1 is able to capture the full strength of climate trends in its observations because the reanalysis assimilates atmospheric temperatures and other observations that are affected by the greenhouse gases and aerosols (14). Peterson (9) and Vose *et al*. (15) also pointed out that the lack of adjustments for inhomogeneity caused by the nonclimatic effects in the observational data may have introduced uncertainties in the UHI estimate of Kalnay and Cai (7).

Here we adopt the method of Kalnay and Cai (7) to estimate the impact of urbanization and other land-use changes on climate in China but pay more attention to the aforementioned problems. We use observed monthly mean daily maximum and minimum land surface air temperatures at 671 meteorological stations of the Chinese network for the period from January 1979 to December 1998, collected and processed by the National Meteorological Center of the China Meteorological Administration (16). We use the National Centers for Environmental Prediction/Department of Energy (NCEP/DOE) Atmospheric Model Intercomparison Project (AMIP)-II Reanalysis (R-2) (11) covering 1979–present at spatial resolution of ≈1.9° instead of R-1. R-2 data were provided by the National Oceanic and Atmospheric Administration/Cooperative Institute for Research in Environmental Sciences (NOAA/CIRES) Climate Diagnostics Center (Boulder, CO) from www.cdc.noaa.gov. Although based on the widely used R-1, the R-2 has improved its quality by featuring newer physics and observed soil moisture forcing and also by fixing known errors of R-1. For example, the soil wetness evolution is treated completely differently in R-2 than in R-1, and a new cloudiness-relative humidity table is generated to fix the errors in R-1. Consequently, the R-2 data should more accurately characterize soil moisture, cloud, and near surface temperature over land (11). To ensure the reliability of R-2 data, we assess the performance of R-2 temperatures relative to observational data and locate the regions and seasons with the best consistency by considering China's complex topography and climate. To minimize the nonclimatic effects in the observations, we use China's original and homogeneity-adjusted annual mean surface air temperature data (17) to assess the magnitude of these effects across China and choose our study region where such effects are minimal. Furthermore, we use independent data sources from demography and remote sensing to further confirm our results. Details about these procedures can be found in the supporting information.

For each meteorological station, the maximum and minimum temperatures in R-2 are interpolated to its location (longitude and latitude) on the R-2 grid. We aggregate the R-2 data into monthly mean values and calculate a monthly DTR by subtracting the monthly mean minimums from the maximums for both the observational and R-2 data. Monthly anomalies then are calculated by removing the 20-year mean annual cycle. Linear trends for both observed and R-2 data are estimated by using ordinary least squares.

After carefully assessing the data quality, reliability, and homogeneity for both observational and R-2 data, we focus our study on 13 provinces and municipalities in southeast China (20°N–36°N, 102°E–123°E) that consist of 194 spatially well distributed stations, representing an area where most of China's urbanization has occurred (18, 19). This region has (*i*) the highest meteorological station density; (*ii*) the most uniform station distribution; (*iii*) the minimal nonclimatic effects; and (*iv*) the best consistency between observations and R-2 data in China. The details are described in the supporting information.

Fig. 1 shows time series of monthly temperature anomalies for Shenzhen, a city with the fastest population growth in China from ≈0.1 million in 1982 to ≈7 million in 2000. The R-2 data are consistent with meteorological observations, with a correlation coefficient of 0.78 and 0.85 for maximum and minimum temperatures, respectively. The minimum temperature in the meteorological data has a larger warming trend than the maximum does, and so DTR decreases (−0.62°C per decade). This change is consistent with commonly reported UHI (20, 21), which has the greatest effect on the minimum temperature. In contrast, the R-2 DTR shows a small increase (0.09°C per decade), suggesting a lower sensitivity to urbanization. Therefore, the observed minus R-2 temperature trends can be largely attributed to urbanization and other land-use changes (7, 14).

To estimate the overall trends over our study region, we average all stations, giving each equal weight because of their uniform distribution in space. Because the R-2 data show the best quality relative to the observational data during winter months (December–February), which is also the season when the cloudiness and soil moisture effects on UHI are minimal both for the R-2 and observations (see more in the supporting information), results in the winter months are show below.

For further information on data, procedures, and results for other seasons, see *Supporting Text*, Tables 1–3, and Figs. 6–15, which are published as supporting information on the PNAS web site.

GEOPHYSICS

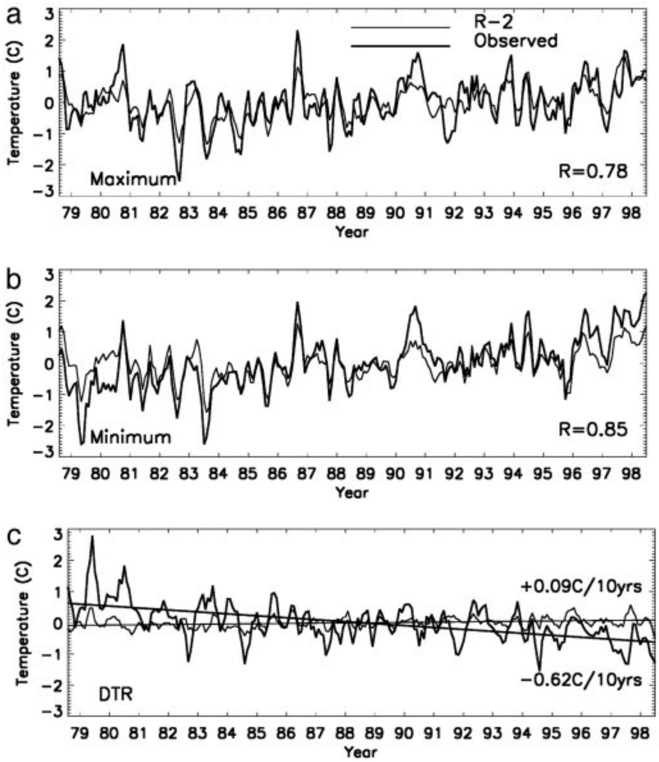

Fig. 1. Monthly temperature anomalies in the observational and R-2 data for Shenzhen, a city with the fastest population growth in China, from January 1979 to December 1998: maximum (*a*), minimum (*b*), and DTR (*c*). A 3-month smoothing is applied. The correlation coefficient between the two data sets (without smoothing) is shown.

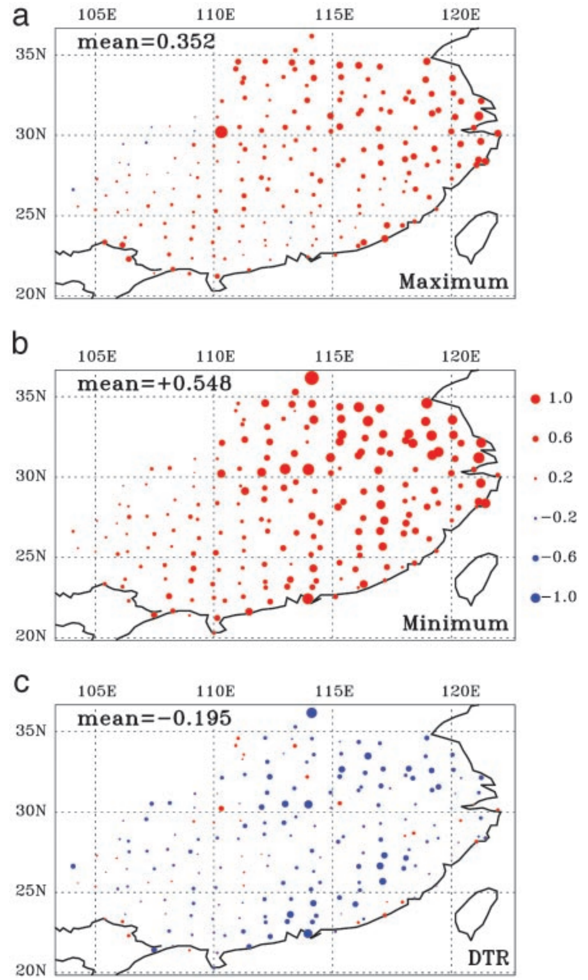

Fig. 2. Observed winter temperature trends (in °C per decade) over southeast China from 1979 to 1998: maximum (*a*), minimum (*b*), and DTR (*c*).

Results and Discussion

Trends for winter maximum and minimum temperatures and DTR in the observations are shown in Fig. 2. On average, the observed maximum and minimum temperatures increase by 0.352°C and 0.548°C per decade, respectively, and the DTR decreases by 0.195°C per decade. The daily minimum rises faster than the daily maximum, with the largest increase in the northern and eastern areas of the study region. Consequently, the DTR declines at a majority of stations, with the largest decrease in the eastern and southern coastal areas where rapid urbanization has occurred (18, 19).

Fig. 3 shows how much of the above observed temperature changes can be attributed to urbanization and other land-use changes. The average differences in maximum and minimum temperature trends between observed and R-2 data are −0.016 and 0.116°C per decade, respectively. The difference in DTR trend is −0.132°C per decade, which is 68% of the observed DTR trend (−0.195°C per decade). The decrease of DTR is greatest in the Yangtze and Pearl River deltas and generally is larger at coastal stations. Note that most Chinese stations are located in or near cities. The spatial pattern and magnitude of changes in the DTR generally are consistent with several indicators for urbanization (e.g., number of towns and cities, urban population, rural–urban migrants, rural laborers transferred to nonagricultural sectors, rural–urban income, and per capita gross domestic product) (19). Consequently, we attribute most of the changes shown in Fig. 3 to urbanization.

The DTR is particularly susceptible to urban effect (1). If urbanization is responsible for the reduction in DTR, changes in DTR (Fig. 3*c*) should be correlated with factors known to affect urbanization. The percentage of urban population to the total population (referred to as percentage urban hereafter) has been used as the most important determinant of urbanization in China (19). We use China's fourth (1990) and fifth (2000) census data (22) to measure the changes in percentage urban. The DTR trends are aggregated to the provincial level because data at station level are not available to us. Fig. 4*a* shows a statistically significant negative correlation (-0.77, $p < 0.01$) between changes in DTR and those in percentage urban. Areas with the greatest increase in percentage urban have the largest reduction in DTR.

Changes in satellite-measured greenness are another indicator of urbanization. Vegetation greenness indices such as the normalized difference vegetation index (NDVI) use red and near-infrared solar radiation reflected back to sensors aboard satellites to signal energy absorption by leaf pigments such as chlorophyll (23). Reflectances for vegetated and urban surfaces differ greatly, and so decreases in NDVI indicate the occurrence of less vegetation. Such decreases should be most pronounced and thus best seen during summer, when vegetation peaks, and become smallest during winter, when the bare soil fraction is largest because urban surfaces are similar to bare soil in their reflectance spectrum. Therefore, we estimate summer NDVI trends for each station with an 8-km resolution data set (23) from 1982 to 1998 as we did for the R-2 data.

The spatial pattern and magnitude of summer NDVI trends (Fig. 5) are generally consistent with those in temperatures (Fig. 3) and land use in China. Satellite greenness decreases substan-

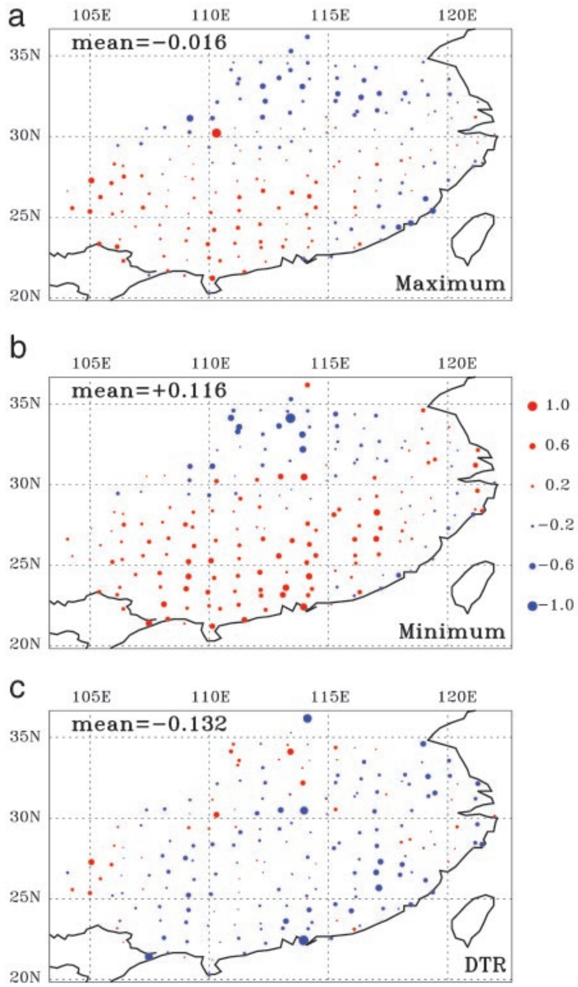

Fig. 3. Observed minus R-2 winter temperature trends (in °C per decade) in southeast China from 1979 to 1998: maximum (*a*), minimum (*b*), and DTR (*c*).

tially over the eastern and southern provinces but increases over the important agricultural areas of northern and western provinces (30°N–35°N). Variations in NDVI exhibit the greatest association with the UHI effect for minimum temperature (see Table 3), as shown in Gallo and Owen (8). The correlation coefficients between changes in NDVI and the observed minus R-2 minimum temperature trends are −0.30 ($p < 0.01$, sample = 194) at station level and −0.67 ($p < 0.05$, sample = 13; Fig. 4*b*) at provincial level.

Use of remote sensing data for detecting urbanization generally requires fine-resolution (<1 km) imagery (24). Note that the size of NDVI pixel (64 km^2) used in this study is coarse relative to that of most cities, especially in the agricultural region. The observed NDVI changes may contain signals other than urbanization, which could vary by station depending on its location relative to the center of NDVI pixel. Hence, the correlation at provincial level may be more representative of urbanization than that at station level because the regional average could reduce uncertainty.

Although a substantial conversion from arable land into built-up areas was identified (25), the observed NDVI increase in 30°N–35°N (Fig. 5) may reflect the climatic effects of both urbanization and increased agricultural planting around the cities, because a substantial rise in crop yield has been reported attributable to increased irrigation and fertilizer application from 1982 to 1999 (26) over this agricultural region. Such an

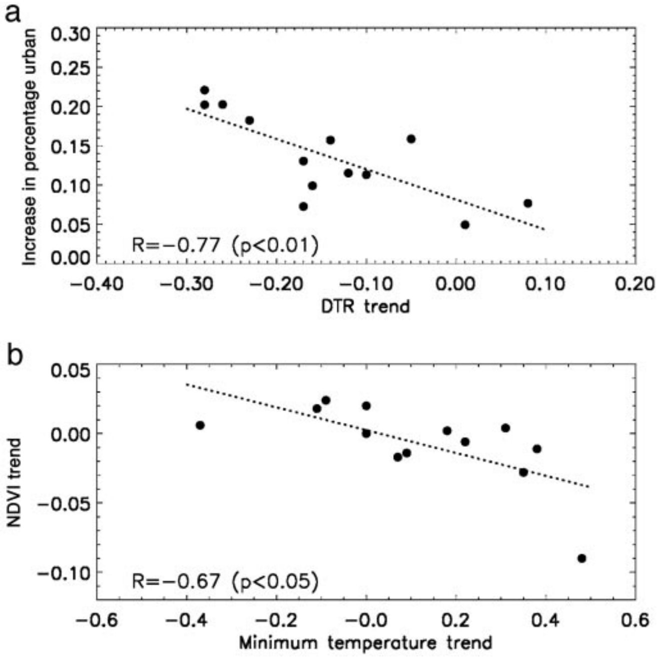

Fig. 4. Relationship for the DTR trends (in °C per decade; Fig. 3*c*) versus the increases in percentage urban (*a*) and the minimum temperature trends (in °C per decade; Fig. 3*b*) versus summer greenness trends (per decade; Fig. 5) at provincial level (*b*). The correlation coefficients and their significance level are shown. The dashed line represents a least-squares fit.

increase over urban areas coincides with the decline in maximum and minimum temperatures (Fig. 3), suggesting a cooling urban effect caused by enhanced evapotranspiration (4, 27). Apparently, the UHI is very complicated and site-dependent.

We also calculate the correlation coefficients like Fig. 4 *a* and *b* for other seasons and find that winter is the most reliable season to estimate the UHI effect in China (see more in the supporting information), consistent with (*i*) the relationship between changes in DTR and those in percentage urban, (*ii*) the relationship between trends in minimum temperature and those in NDVI, and (*iii*) the seasonal variations of the R-2 data quality relative to the observational data. Our results also are consistent with the UHI mechanisms (20, 21). Urban and rural areas may differ in cloud cover and rainfall, and this difference should be largest in summer, especially for a marked monsoon climate country like China. Therefore, the UHI should be expected more visible in winter than in summer when both clouds/rainfall and UHI decrease DTR and thus cannot be differentiated in the observations.

The impact of urbanization on climate over our study region is computed by using the observed minus R-2 trend for mean

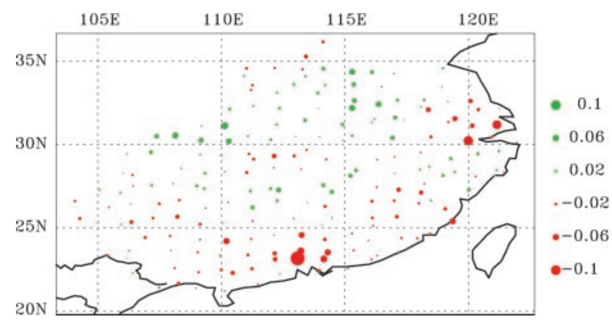

Fig. 5. Summer NDVI trends per decade from 1982 to 1998.

GEOPHYSICS

winter surface temperature averaged from the maximum and minimum values. Our estimated warming of mean surface temperature of 0.05°C per decade is much larger than previous estimates (1–7) for other periods and locations, including the estimate of 0.027°C for the continental U.S. (7). A recent study by Li *et al*. (28) finds that most temperature time series in China are affected by UHI, and they estimated the UHI over our study region of ≈0.011°C per decade based on analyses of the rural–urban differences in annual mean temperature for the period of 1951–2001. Because the present analysis is from the winter season over a period of rapid urbanization and for a country with a much higher population density, we expect our results to give higher values than those estimated in other locations and over longer periods. Therefore, our estimates do not represent the urbanization effect globally, nor do they represent the average of all seasons over the past 100 years for which station temperature data are available.

Some uncertainties may still remain in our estimates, such as the previously discussed nonclimatic effects. To estimate such effects over our study region, we use the original and homogeneity-adjusted annual mean temperature data (28) to compute the difference in temperature trend before and after the adjustments (see more in the supporting information). The regional average difference is 0.002°C per decade, indicating a minimal effect on our estimated UHI. Considering the complexity of the UHI that involves many nonurban impacts, such as incomplete adjustments of data inhomogeneity (9, 15), clouds (4, 13), aerosols (29) (which are largest during spring), and changes in solar radiation and insolation duration (30, 31), our results should be interpreted as illustrative rather than definitive. However, this study draws attention to an important issue that requires further investigation. We need to better characterize the system with observations and better describe and model the complex processes involved. This article is a first step in the development of a quantitative basis for assessing the consequences from temperature of land-use change associated with Chinese urbanization.

We are grateful to reviewers for their constructive suggestions that have improved this manuscript significantly. This study was supported by National Aeronautics and Space Administration Earth Science Enterprise.

1. Intergovernmental Panel on Climate Change (2001) in *Climate Change 2001: The Scientific Basis*, eds. Houghton, J. T., Ding, Y., Griggs, D. J., Noguer, M., van der Linden, P. J., Dai, X., Maskell, K. & Johnson, C. A. (Cambridge Univ. Press, Cambridge, U.K.).
2. Jones, P. D., Groisman, P. Ya., Coughlan, M., Plummer, N., Wang, W.-C. & Karl, T. R. (1990) *Nature* **347,** 169–172.
3. Easterling, D. R., Horton, B., Jones, P. D., Peterson, T. C., Karl, T. R., Parker, D. E., Salinger, M. J., Razuvayev, V., Plummer, N., Jamason, P., *et al*. (1997) *Science* **277,** 364–367.
4. Karl, T. R., Jones, P. D., Knight, R. W., Kukla, G., Plummer, N., Razuvayev, V., Gallo, K. P., Lindseay, J., Charlson, R. J. & Peterson, T. C. (1993) *Bull. Am. Meteorol. Soc.* **74,** 1007–1024.
5. Hansen, J., Ruedy, R., Sato, Mki., Imhoff, M., Lawrence, W., Easterling, D., Peterson, T. & Karl, T. (2001) *J. Geophys. Res.* **106,** 23947–23963.
6. Gallo, K. P., Owen, T. W., Easterling, D. R. & Jamason, P. F. (1999) *J. Clim.* **12,** 1344–1348.
7. Kalnay, E. & Cai, M. (2003) *Nature* **423,** 528–531.
8. Gallo, K. P. & Owen, T. K. (1999) *J. Appl. Meteor.* **36,** 806–813.
9. Peterson, T. C. (2003) *J. Clim.* **16,** 2941–2959.
10. Kistler, R., Kalnay, E., Collins, W., Saha, S., White, G., Woollen, J., Chelliah, M., Ebisuzaki, W., Kanamitsu, M., Kousky, V., *et al*. (2001) *Bull. Am. Meteorol. Soc.* **82,** 247–268.
11. Kanamitsu, M., Ebisuzaki, W., Woollen, J., Yang, S.-K., Hnilo, J. J., Fiorino, M. & Potter, G. L. (2002) *Bull. Am. Meteorol. Soc.* **83,** 1631–1643.
12. Trenberth, K. E. (2004) *Nature* **427,** 213–213.
13. Dai, A., Genio, A. D. Del & Fung, I. Y. (1997) *Nature* **386**, 665–666.
14. Cai, M. & Kalnay, E. (2004) *Nature* **427,** 214.
15. Vose, R. S., Karl, T. R., Easterling, D. R., Williams, C. N. & Menne, M. J. (2004) *Nature* **427,** 214.
16. Fang, J. Y., Piao, S. L., Tang, Z. Y., Peng, C. H. & Ji, W. (2001) *Science* **293,** 1723.
17. Li, Q., Liu, X., Zhang, H., Peterson, T. C. & Easterling, D. R. (2004) *Adv. Atmos. Sci.* **21,** 1–9.
18. Seto, K. C., Kaufmann, R. K. & Woodcock, C. E. (2000) *Nature* **406,** 121.
19. Liu, S., Li, X. & Zhang, M. (2003) in *Scenario Analysis on Urbanization and Rural–Urban Migration in China*, Interim Report IR-03-036 (International Inst. for Applied Systems Analysis, Vienna, Austria), www.iiasa.ac.at/Publications/Documents/IR-03-036.pdf.
20. Oke, T. (1987) *Boundary Layer Climates* (Methuen, London).
21. Arnfield, A. J. (2003) *Int. J. Climatol.* **23,** 1–26.
22. Lavely, W. (2001) *Popul. Dev. Rev.* **27,** 755–769.
23. Zhou, L., Tucker, C. J., Kaufmann, R. K., Slayback, D., Shabanov, N. V. & Myneni, R. B. (2001) *J. Geophys. Res.* **106,** 20069–20083.
24. Carlson, T. (2003) *Remote Sens. Environ.* **86,** 273–274.
25. Liu, J., Liu, M., Zhuang, D., Zhang, Z. & Deng, X. (2003) *Sci. China D* **46,** 373–384.
26. Editorial Committee for China's Agricultural Yearbook (2000) *China's Agricultural Yearbook 1999* (Agriculture Press, Beijing).
27. Bounoua, L., Collatz, G. J., Los, S. O., Sellers, P. J., Dazlich, D. A., Tucker, C. J. & Randall, D.A. (2000) *J. Clim.* **13,** 2277–2292.
28. Li, Q., Zhang, H., Liu, X. & Huang, J. (2004) *Theor. Appl. Climatol.*, in press.
29. Luo, Y., Lu, D., He, Q., Li, W. & Zhou, X. (2000) *Chinese Sci. Bull.* **45,** 1328–1333.
30. Li, X., Zhou, X., Li, W. & Chen, L. (1995) *Acta Meteorolog. Sinica* **9,** 57–68.
31. Chen, L., Zhu, W., Wang, W., Zhou, X. & Li, W. (1998) *Acta Meteorolog. Sinica* **12,** 1–17.

Supporting Text

Chinese Meteorological Station Network

The Chinese observed land-surface air temperature data set includes measurements from 731 meteorological stations from 1951 to the present, as collected and processed by the National Meteorological Center of the China Meteorological Administration (1, 2). Because some stations were removed, the actual total number of stations in operation today is 671, distributed among 31 provinces and municipalities. Fig. 6 shows the district map of these provinces and municipalities, and Fig. 7 shows the location and topography of these stations. In this study, we use the monthly mean daily maximum and minimum temperature data (1) from the 610 stations that have a complete set of observations for the period from January 1979 to December 1998.

China, with a population of ≈1.3 billion and an area of 9.6×10^6 km^2, has a complex topography. Its terrain descends gradually from west to east like a staircase, with the towering Tibetan plateau called the "roof of the world" to the west and the flat and fertile plains to the eastern coast of the Pacific Ocean. From north to south, the elevation drops from 1,000–2,000 m of the Inner Mongolia Plateau to <200 m of southeast China. This varied topography is associated with a large gradient in climate. China has a marked continental monsoon climate, with cold and dry winters and hot and humid summers, especially in southeast China. Northerly winds prevail in winter, whereas southerly winds reign in summer. The warm and moist summer monsoons from the oceans bring abundant rainfall and high temperatures to most of China. Annual precipitation varies greatly from <50 mm in Northwest China to ≈3,000 mm in southern China (1).

Problems in Estimating UHI Effects by Using Observational Data

The UHI effect has been estimated by using *in situ* observations around the world, mostly by comparing observed temperatures in urban stations with those from surrounding rural stations (3, 4). The estimated UHI varies significantly by region, time, and method. In the

U.S., the estimated UHI varies from 0.06°C to 0.15°C per century, depending on whether population data or satellite measurements of night lights are used to classify urban versus rural stations (5, 6). In contrast, Peterson (4) finds that the UHI has no significant impact on temperature in the U.S. after observed temperatures are adjusted for inhomogeneities caused by "nonclimatic" factors such as changes in location (altitude and latitude), observation time, instrumentation, and nonstandard siting. These nonclimatic factors could introduce artifacts in long-term observations and rural–urban differences and thus may bias the estimate of UHI. The lack of an UHI effect may be caused by micro- and local-scale impacts overwhelming the mesoscale UHI. Industrial sections of towns may well be significantly warmer than rural sites, but urban meteorological observations are more likely to be made within cool "park islands" than industrial regions (4). Evidently, the UHI is more complex than usually considered.

Using temperature differences between urban and rural stations to estimate the UHI effect in China may be inappropriate (7) for several reasons. First, most Chinese stations are located in or near cities, with only a few in mountainous or remote regions or on small islands. For example, the China's Fifth (2000) Census indicates that only 27% of Chinese meteorological stations have a permanent urban population <10,000, and these stations are located mostly in west China [Q. Li (China's National Meteorological Center) personal communication]. Although China is comparable in size to the U.S., it has considerably fewer meteorological stations and each city generally has only one station. For example, China's two biggest cities, Beijing and Shanghai, each has only one station available in the Chinese network. Kalnay and Cai (8) used nearly 2,000 meteorological stations for the continental U.S. in their study. It is impossible to find a corresponding rural station for most of the urban ones, especially in eastern and southern China. Consequently, if using the rural–urban difference to estimate the UHI, one possibly is comparing temperature between two different urban stations at regional scales or between two different regions at large scales. For this reason, Li *et al*. (7) divided China into five subregions and estimated their UHI effect separately. Furthermore, adjusting spatial and temporal homogeneities for *in situ* observations in China may inadvertently sacrifice the UHI effect because the adjustments often are performed by comparing a target station with its neighbors that generally are also urban stations and relatively far away. Second, China's rapid urbanization in the past two decades could transfer a station from rural into urban in a very short period. The continuous expansion in urban population and area makes the classification of urban versus rural station dynamic. Third, Chinese cities have a much higher density of population and urban buildings than do cities in most developed countries. Cities in the U.S. extend many kilometers to suburban areas where people reside and that can have as much vegetation as rural areas, whereas Chinese cities have a significantly higher density of population, residential buildings, shopping malls, schools, roads, etc., and much less vegetation than their neighboring rural areas do because people live within cities. These unique characteristics could make the UHI effect more pronounced in China than in other countries like the U.S.. For example, after the homogeneity adjustments to China's mean surface temperature, Li *et al*. (7) find that most Chinese temperature time series are inevitably affected by UHI.

Homogeneity Assessment of Observational Data

The central problem with any long-term analysis of climate data is that inhomogeneities, which are caused by several factors such as changes in location, observing practices, instrumentation, and nonstandard siting (4, 9, 10), could introduce large biases in the data and thus lead to inaccurate or erroneous conclusions. Several techniques have been introduced to remove these factors (9). They generally compare a reference series against a candidate time series to test for inhomogeneities. The reference series is created by using neighbor stations to establish an ideal, completely homogenous series. The candidate series then is adjusted by comparison with this reference series. Currently, the Global Historical Climatology Network (GHCN) (11) and the U.S. Historical Climatology Network (USHCN) (12) are two homogeneity-adjusted time series at large scale for long-term climate analysis. However, the GHCN data set could not be used in this study because most of the data between 1979 and 1998 are not available over China.

Recently, Li *et al.* (2) adopted the Easterling–Peterson (E-P) techniques (12) to test Chinese meteorological observations for inhomogeneities in historical mean surface air temperature series from 1951 to 2001. The results indicate that the time series have been affected greatly by inhomogeneities due to the station relocation and other nonclimatic effects. Based on the amplitude of changes in the first difference of the time series and the monthly distribution features of surface air temperatures, discontinuities identified by applying the E-P technique supported by China's metadata, or by comparison with other approaches, have been adjusted. The inhomogeneity testing detects most nonclimatic changes and indicates that the adjusted data has been largely improved in its reliability and could help decrease uncertainties in the study of observed climate change in China.

Here we cannot make the same adjustments to the maximum and minimum temperature time series used in this study because the China's National Meteorological Center does not allow foreign scientists access to the required metadata. Instead, we use the latest homogeneity-adjusted mean surface temperature data set of Li *et al.* (2) to assess the magnitude of nonclimatic effects in China. Fig. 8 shows the total number of main discontinuities in the annual mean air temperature for each station during the period 1951–2001 due to station relocations and other nonclimatic effects. Most discontinuities are located in north and west China, with only fewer in southeast China, and some stations have up to six discontinuities. Fig. 9 illustrates the long-term trends of annual mean temperature before and after the adjustment. Significant adjustments are observed in Qinghai, North China, Tibet, and Sichuan. Evidently, the homogeneity adjustments are minimal in southeast China.

Quality Assessment of R-2 Data

Kalnay and Cai (8) estimate the impacts of urbanization and other land-use changes on climate based on the difference in surface temperature trends between meteorological observations at 1,982 surface stations in the continental U.S. and NCEP/NCAR Reanalysis (R-1) (13). The R-1 uses the most extensive observations available from a variety of sources including ship, rawinsonde, pibal, aircraft, and satellite, etc., to assimilate these data with an assimilation system kept unchanged. The R-1 data are strongly influenced by atmospheric vertical soundings of wind and temperature, and surface temperatures are estimated from the atmospheric values (surface observations of temperature, moisture, and wind over land are not used) and thus are insensitive to changes in land surface (8). Therefore, the differences in surface temperature trends between meteorological observations and R-1 are postulated to represent the impacts of urbanization and other land-use changes on climate.

This method assumes that the quality of R-1 surface air temperatures is satisfactory. One known deficiency with R-1 data is its poor performance in the description of cloudiness and surface moisture, which could bias the computation of the surface energy budget and thus surface air temperature (14, 15). Increased cloud cover is linked with the worldwide decline in DTR, and increased soil moisture could reduce DTR through enhanced evapotranspiration (14–16). Consequently, differences in clouds and soil moisture between observed and R-1 data could contaminate the UHI estimate. The second deficiency with R-1 data is its poor performance over mountainous regions (8). The model of R-1 has a spatial resolution of 2.5° and thus uses a land-surface boundary that is smoother than reality. This smoothing could introduce large biases in the model's altitude or land-surface properties relative to the actual meteorological stations and thus in the R-1 temperatures over mountainous areas with varied topography. Vose *et al.* (10) and Peterson (4) point out the lack of inhomogeneity adjustments in the observational data in the study of Kalnay and Cai (8). Trenberth (15) argues that the R-1 does not include effects of changing atmospheric composition such as greenhouse gases and aerosols on radiative forcing, but Cai and Kalnay (17) have shown in their reply that the R-1 data are able to capture the full strength of climate trends because the reanalysis assimilates atmospheric temperatures and other observations that are affected by the greenhouse gases and aerosols.

Here we adopt the method of Kalnay and Cai (8) to estimate the impact of urbanization and other land-use changes on climate in China but pay more attention to the aforementioned problems. We choose the NCEP/DOE AMIP-II Reanalysis (R-2) (14) covering 1979–present at spatial resolution of ≈1.9° instead of R-1. Although based on the widely used R-1, the R-2 has improved its quality by featuring newer physics and observed soil moisture forcing and also by fixing known errors of R-1. For example, the soil wetness evolution is treated completely differently in R-2 than in R-1, and a new cloudiness-relative humidity table is generated to fix the errors in R-1. Consequently, the R-2 should more accurately characterize soil moisture, cloud, and near surface temperature over land (14).

One way to evaluate the accuracy of R-2 data is to compare the time series of monthly maximum and minimum temperature anomalies with observed data. We calculate the correlation coefficient between the two data sets for both maximum and minimum temperatures for all stations. If the R-2 captures well the observed surface temperature variations due to changes in weather systems, they should be highly correlated. Fig. 10 shows the spatial pattern of correlation coefficients between the R-2 and observed time series of maximum and minimum temperatures. Evidently, the correlation coefficients are greatest for southeast China, followed by north China, whereas west China has the smallest correlation coefficients. This pattern corresponds with China’s topography. The smallest correlation is observed at some stations in Tibet, Sichuan, and Yunnan provinces, where the topography is highly variable. Similar results also are found for several stations located on high mountains or islands in east China. These results suggest that the quality of the R-2 data need to be checked before it can be used in climate studies.

Choosing Our Study Region

To ensure the reliability of our analyses, we choose our study region carefully based on the quality, reliability, and homogeneity of the observational and R-2 data as described above. Our study region should have the smallest nonclimatic effects in the observations and the highest correlation coefficients between the observed and R-2 data. It also should include the area where most of China’s urbanization has occurred. China has experienced a slow urbanization due to its special political, social, and economic circumstances before its reforms in 1978 (18). Since then, its rapid urbanization has been very inhomogeneous and occurred mainly in southern and eastern provinces, with the fastest economic growth near the Yangtze and Pearl River deltas (19).

Evidently, these requirements are satisfied by southeast China. This region includes twelve provinces (Anhui, Guangdong, Guangxi, Jiangsu, Jiangxi, Henan, Zhejiang, Hubei, Hunan, Fujian, Guizhou, and Hainan) and two municipalities (Shanghai and Chongqing). We eliminated the Hainan province from this study, which consists of islands surrounded by oceans, and several stations located on mountains and small islands in other provinces for two reasons. One is the difference in altitude and land-surface properties between the coarse resolution R-2 data and the observations. The second is that the size of some islands is smaller than that of NDVI pixels (64 km^2), which have observations only over land. Consequently, we focus our study on southeast China (20°N–36°N, 102°E–123°E), consisting of 194 spatially well distributed stations and representing an area where most of China's urbanization has occurred (18). This region has (*i*) the highest meteorological station density; (*ii*) the most uniform station distribution; (*iii*) the minimal nonclimatic effects; and (*iv*) the best consistency between the observed and R-2 data in China.

Following Kalnay and Cai (8), we also test the sensitivity of the R-2 data to urbanization by comparing the annual mean temperature trends between urban and rural stations classified based on population data. Because only cities with populations larger than 100,000 are available from the China's Fourth (1990) Census (United Nations, *Population of Capital Cities and Cities of 100,000 and More Inhabitants: China*, available online from http://unstats.un.org/unsd/citydata/default.asp?cid = 157), we adopt a threshold of 100,000 instead of 50,000 or less, a criterion that is often used to differentiate between an urban or nonurban station (5, 6, 20, 21), to classify all 194 stations into two categories: 109 (rural) and 85 (urban). The annual mean temperature trend (in °C per decade) and its standard deviation are 0.27 ± 0.23 for rural stations and 0.30 ± 0.21 for urban stations in the R-2 data. In the observations, the corresponding values are 0.32 ± 0.21 and 0.39 ± 0.21, respectively. The rural–urban difference is statistically significant at the 5% level for the observations (0.07) but insignificant for the R-2 (0.03), indicating small sensitivity of the latter to UHI.

As discussed previously, using the rural–urban temperature difference may be inappropriate to estimate the UHI in China. For example, the above estimated rural–urban difference in the observational data may not represent the UHI effect because the majority of urban stations classified above are located in the coastal provinces, whereas most of the rural stations are located in the northwestern provinces. In other words, it may represent the temperature differences between the two regions rather than the differences between urban stations and their rural counterparts.

Seasonal Variations in Observed and R-2 Temperature Trends

Although the R-2 data are based on a better description of cloudiness and soil wetness, some uncertainties may still remain regarding the complexity of China's topography and climate. We examine the consistency of R-2 and observational data over our study region by season: winter (December–February), spring (March–May), summer (June–August), and autumn (September–November). Fig. 11 shows the histogram for the correlation coefficient between the R-2 and observed data for both maximum and minimum temperatures by season. Evidently, the R-2 shows the best consistency with the observational data during winter, followed by autumn, spring, and summer. The weakest consistency in summer indicates that the R-2 temperatures may be still biased by its incomplete cloud and soil moisture description. These results imply that the winter R-2 data will generate the most reliable estimate for the UHI effect.

The UHI effect in China is largest during spring based on analyses of *in situ* observations by using the rural–urban differences [Q. Li, (China's National Meteorological Center), personal communication], but spring corresponds to the largest aerosol effect (22). Therefore, we use the winter temperature data to estimate the urbanization effect on climate in China. Winter is also the season when the effects of clouds and soil wetness are smallest for observational data. Increased cloud cover has been linked with the worldwide decline in DTR (16). Urban and rural areas may differ in cloud cover and rainfall, and this difference should be largest in summer, especially in a marked monsoon climate country like China. Therefore, the UHI should be expected to be more visible in winter than in summer when both clouds/rainfall and UHI decrease DTR and thus cannot be differentiated in the observations.

To estimate the magnitude of the nonclimatic effects over our study region, we use the original and homogeneity-adjusted annual mean temperature data of Li *et al.* (2) to compute the difference in temperature trends for the period of 1979–1998. Our estimate is 0.002°C per decade, indicating the average nonclimatic effect over our study region is small although the homogeneity adjustments could be large for a specific station. This small effect may be, in part, attributed to two factors: (*i*) calibrations are made to most Chinese stations when they are relocated; and (*ii*) the relocations will not produce large differences in altitude and thus in temperatures due to the small variation in elevation over our study region. These results suggest that using the unadjusted data in southeast China will not introduce significant biases.

We also calculate temperature trends and their relation with changes in percentage urban and NDVI for other seasons. Figs. 12–15 show the observed minus R-2 trends for maximum, minimum, and DTR for spring, summer, autumn and annual mean. Table 1 lists seasonal and annual mean temperature trends for the observations, R-2, and their differences. Evidently, the R-2 data for mean temperature has a much smaller trend during summer than in other seasons, resulting in a significant observed minus R-2 mean temperature trend. Table 2 lists the correlation coefficients between changes in percentage urban and observed minus R-2 trends in seasonal and annual DTR trends during the period of 1979–1998. The urban index (i.e., percentage urban) shows the largest correlation with changes in the DTR in winter, followed by autumn, spring, and summer. This ranking is consistent with that in the R-2 data quality in Fig. 11. Table 3 lists the correlation coefficients between summer NDVI trends and observed minus R-2 trends in seasonal and annual mean temperatures during the period of 1979–1998.

Variations in NDVI show the highest correlation with the minimum temperature, as reported in Gallo and Owen (23).

1. Fang, J. Y., Piao, S. L., Tang, Z. Y., Peng, C. H. & Ji, W. (2001) *Science* **293,** 1723.

2. Li, Q., Liu, X., Zhang, H., Peterson, T. C. & Easterling, D. R. (2004) *Adv. Atmos. Sci.* **21,** 1-9.

3. Arnfield, A. J. (2003) *Int. J. Climatol.* **23,** 1-26.

4. Peterson, T. C. (2003) *J. Clim.* **16,** 2941-2959.

5. Hansen, J., Ruedy, R., Sato, Mki., Imhoff, M., Lawrence, W., Easterling, D., Peterson, T. & Karl, T. (2001) *J. Geophys. Res.* **106,** 23947-23963.

6. Gallo, K. P., Owen, T. W., Easterling, D. R. & Jamason, P. F. (1999) *J. Clim.* **12,** 1344-1348.

7. Li, Q., Zhang, H., Liu, X. & Huang, J. (2004) *Theor. Appl. Climatol.*, in press.

8. Kalnay, E. & Cai, M. (2003) *Nature* **423,** 528-531.

9. Peterson, T. C., Easterling, D., Karl, T., Groisman, P., Nicholls, N., Plummer, N., Torok, S., Auer, I., Boehm, R., Gullett, D., *et al*. (1998) *Int. J. Climatol.* **18,** 1493-1517.

10. Vose, R. S., Karl, T. R., Easterling, D. R., Williams, C. N. & Menne, M. J. (2004) *Nature* **427,** 214.

11. Peterson, T. C. & Vose, R. S. (1997) *Bull. Am. Meteorol. Soc.* **78,** 2837-2849.

12. Easterling, D. R. & Peterson, T. C. (1995) *Int. J. Climatol.* **15,** 369-377.

13. Kistler, R., Kalnay, E., Collins, W., Saha, S., White, G., Woollen, J., Chelliah, M., Ebisuzaki, W., Kanamitsu, M., Kousky, V., *et al*. (2001) *Bull. Am. Meteorol. Soc.* **82,** 247-268.

14. Kanamitsu, M., Ebisuzaki, W., Woollen, J., Yang, S.-K., Hnilo, J. J., Fiorino, M. & Potter, G. L. (2002) *Bull. Am. Meteorol. Soc.* **83,** 1631-1643.

15. Trenberth, K. E. (2004) *Nature* **427,** 213.

16. Dai, A., Genio, A. D. Del & Fung, I. Y. (1997) *Nature* **386**, 665-666.

17. Cai, M. & Kalnay, E. (2004) *Nature* **427,** 214.

18. Liu, S., Li, X. & Zhang, M. (2003) in *Scenario Analysis on Urbanization and Rural–Urban Migration in China*, Interim Report IR-03-036 (International Inst. for Applied Systems Analysis, Vienna, Austria), www.iiasa.ac.at/Publications/Documents/IR-03-036.pdf.

19. Seto, K. C., Kaufmann, R. K. & Woodcock, C. E. (2000) *Nature* **406,** 121.

20. Easterling, D. R., Horton, B., Jones, P. D., Peterson, T. C., Karl, T. R., Parker, D. E., Salinger, M. J., Razuvayev, V., Plummer, N., Jamason, P., *et al*. (1997) *Science* **277,** 364-367.

21. Karl, T. R., Jones, P. D., Knight, R. W., Kukla, G., Plummer, N., Razuvayev, V., Gallo, K. P., Lindseay, J., Charlson, R. J. & Peterson, T. C. (1993) *Bull. Am. Meteorol. Soc.* **74,** 1007-1024.

22. Luo, Y., Lu, D., He, Q., Li, W. & Zhou, X. (2000) *Chinese Sci. Bull.* **45,**1328-1333.

23. Gallo, K. P. & Owen, T. K. (1999) *J. Appl. Meteor.* **36,** 806-813.

RUSSIA
KAZAKHSTAN
MONGOLIA
KIRGIZSTAN
XINJIANG
HEILONGJIANG
JILIN
LIAONING
INNER MONGOLIA
Beijing
NORTH KOREA
GANSU
Tianjin
Yellow Sea
PAKISTAN
QINGHAI
HEBEI
SHANXI
NINGXIA
SOUTH KOREA
SHANDONG
Yellow River
CHINA
JIANGSU
HENAN
SHAANXI
TIBET
SHANGHAI
ANHUI
NEPAL
SICHUAN
HUBEI
Yangtze River
ZHEJIANG
East China Sea
BHUTAN
JIANGXI
HUNAN
INDIA
GUIZHOU
FUJIAN
BANGLADESH
YUNNAN
TAIWAN
GUANGXI
GUANGDONG
Hong Kong
BURMA
VIETNAM
South China Sea
LAOS
THAILAND
HAINAN
0
400 km
SCMP Graphic

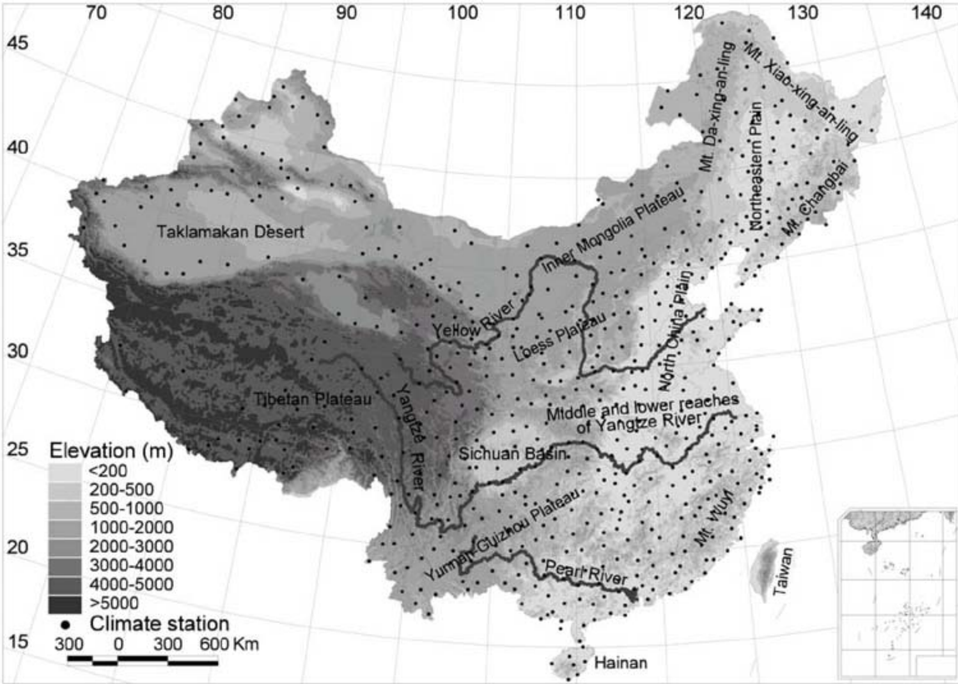
70
80
90
100
110
120
130
140
45
40
35
30
25
20
15
Taklamakan Desert
Tibetan Plateau
Yangtze River
Yellow River
Loess Plateau
Inner Mongolia Plateau
North China Plain
Mt. Da-xing-an-ling
Mt. Xiao-xing-an-ling
Northeastern Plain
Mt. Changbai
Middle and lower reaches of Yangtze River
Sichuan Basin
Yunnan-Guizhou Plateau
Pearl River
Mt. Wuyi
Taiwan
Hainan
Elevation (m)
<200
200-500
500-1000
1000-2000
2000-3000
3000-4000
4000-5000
>5000
Climate station
300 0 300 600 Km

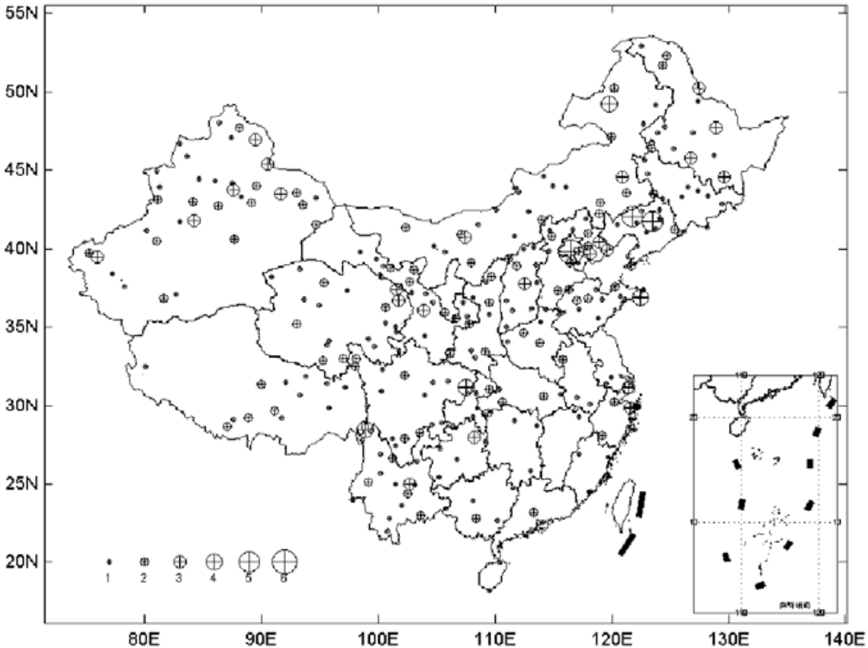
55N
50N
45N
40N
35N
30N
25N
20N
80E
90E
100E
110E
120E
130E
140E
1
2
3
4
5
6

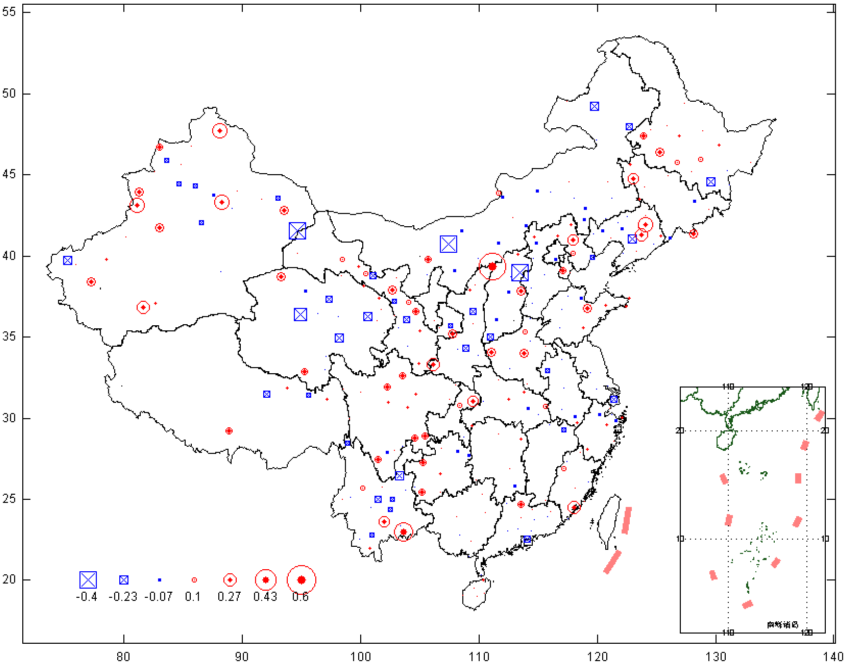

55
50
45
40
35
30
25
20
80
90
100
110
120
130
140
-0.4
-0.23
-0.07
0.1
0.27
0.43
0.6

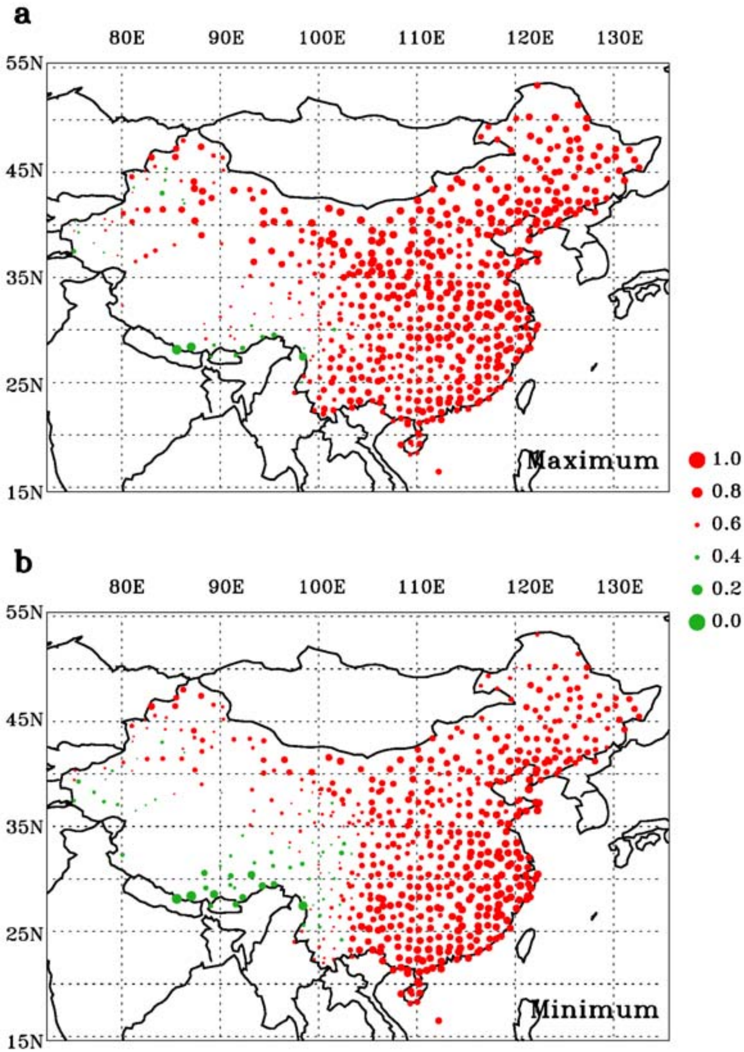
a
80E
90E
100E
110E
120E
130E
55N
45N
35N
25N
15N
Maximum
1.0
0.8
0.6
0.4
0.2
0.0
b
Minimum

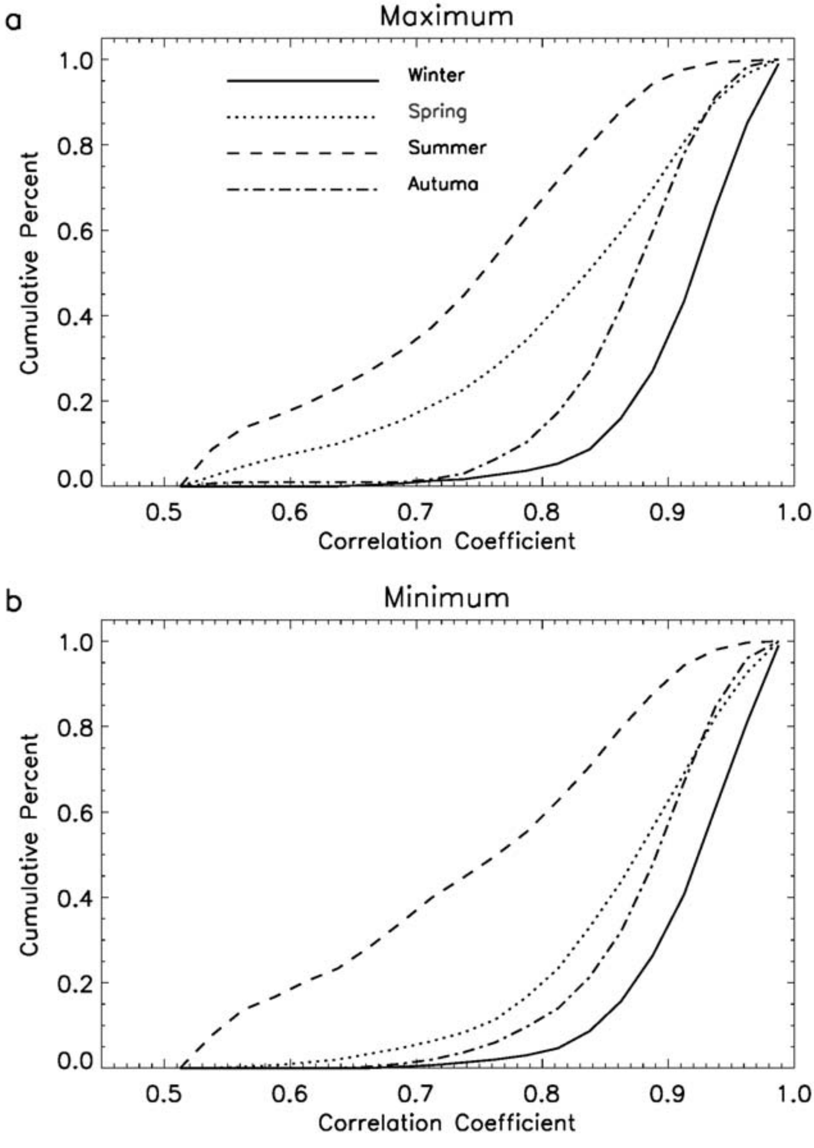
a
Maximum
Winter
Spring
Summer
Autuma
Cumulative Percent
0.0
0.2
0.4
0.6
0.8
1.0
0.5
0.6
0.7
0.8
0.9
1.0
Correlation Coefficient
b
Minimum
Cumulative Percent
0.0
0.2
0.4
0.6
0.8
1.0
0.5
0.6
0.7
0.8
0.9
1.0
Correlation Coefficient

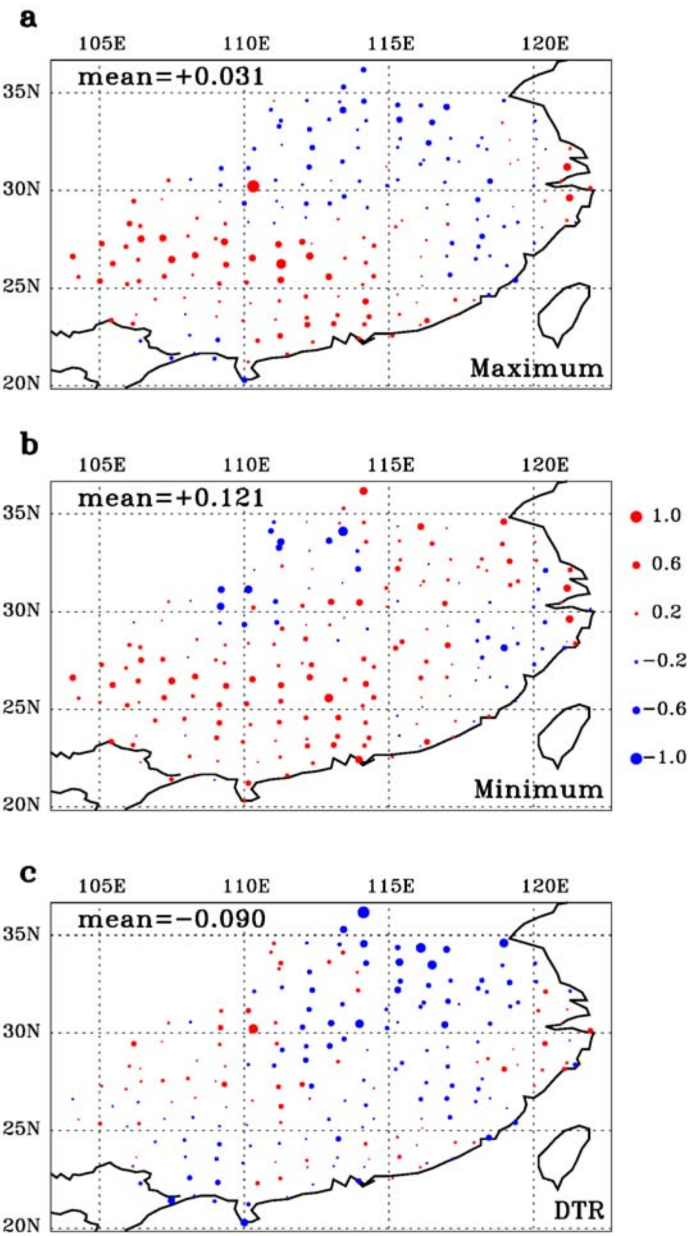
a
105E
110E
115E
120E
mean=+0.031
35N
30N
25N
20N
Maximum
b
mean=+0.121
Minimum
1.0
0.6
0.2
−0.2
−0.6
−1.0
c
mean=−0.090
DTR

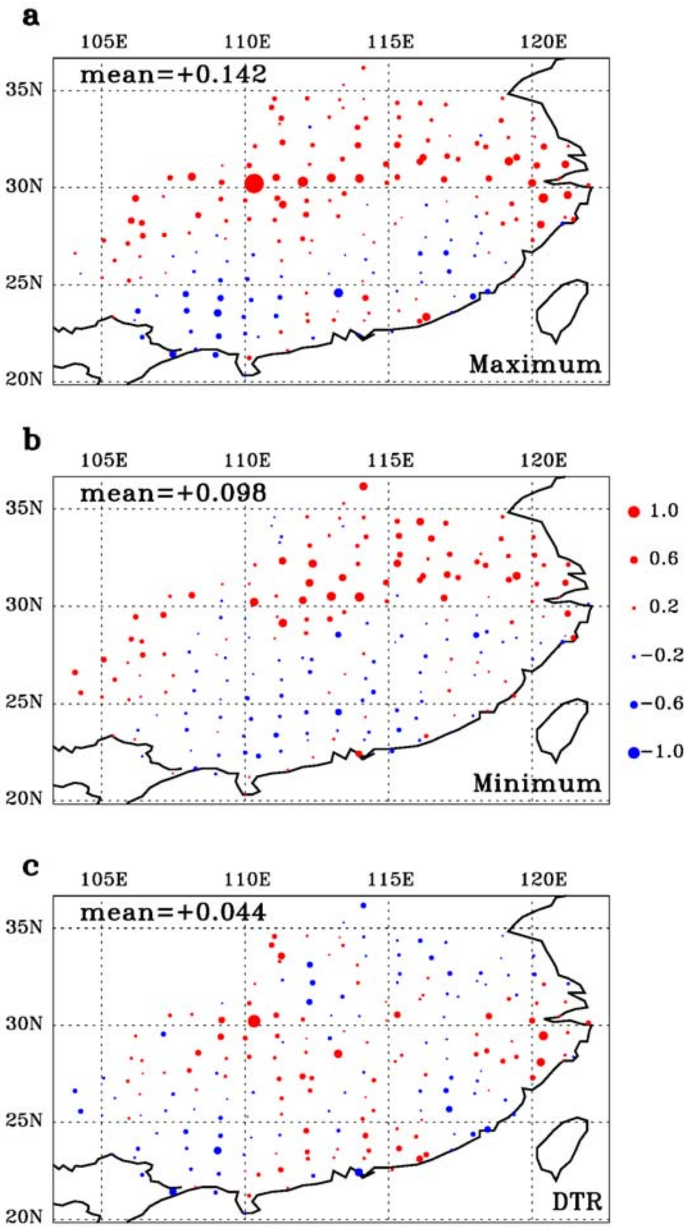
a
105E
110E
115E
120E
35N
30N
25N
20N
mean=+0.142
Maximum
b
mean=+0.098
Minimum
1.0
0.6
0.2
−0.2
−0.6
−1.0
c
mean=+0.044
DTR

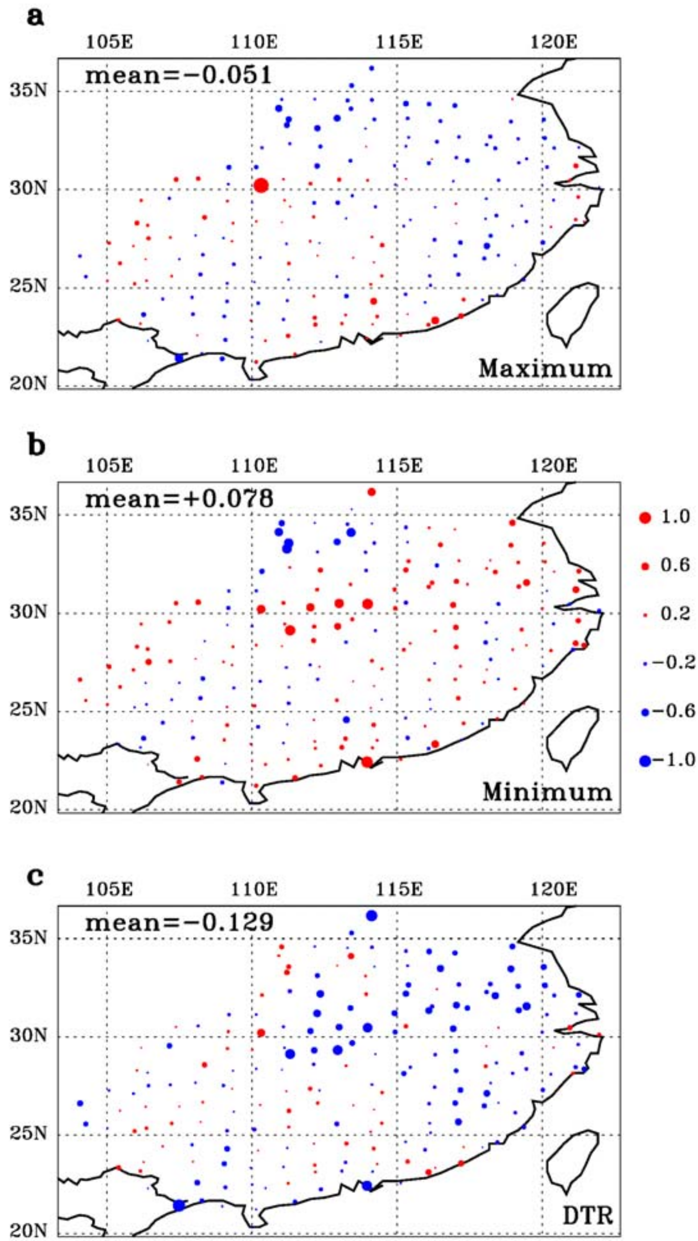
a
mean=−0.051
Maximum
b
mean=+0.078
Minimum
1.0
0.6
0.2
−0.2
−0.6
−1.0
c
mean=−0.129
DTR
105E
110E
115E
120E
20N
25N
30N
35N

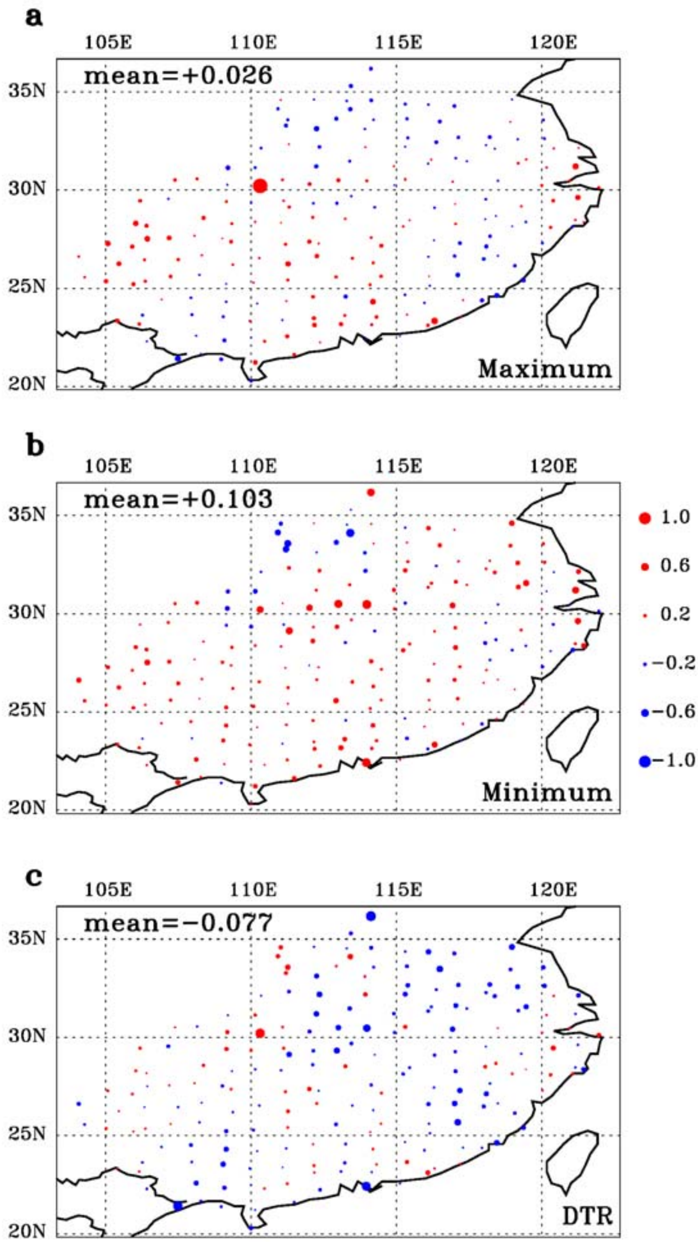
a
105E
110E
115E
120E
35N
30N
25N
20N
mean=+0.026
Maximum
b
mean=+0.103
Minimum
1.0
0.6
0.2
−0.2
−0.6
−1.0
c
mean=−0.077
DTR